Mechanical properties in the physically simulated heat-affected zones of 500 MPa offshore steel for arctic conditions

Henri Tervo[1[0000-0002-2764-6966]], Juho Mourujärvi[1], Antti Kaijalainen[1[0000-0002-1539-2866]], Jukka Kömi[1]

[1] Materials and Production Engineering, P.O Box 4200, FI-90014 University of Oulu, Oulu
henri.tervo@oulu.fi
antti.kaijalainen@oulu.fi
juho.mourujarvi@oulu.fi
jukka.komi@oulu.fi

Abstract. Offshore steels for the arctic conditions have an increasing demand due to the opening of new oil fields in the Arctic Ocean. However, the requirements for these steels are extremely demanding, as they need to maintain the desired properties in harsh arctic conditions. Additionally, these requirements need to be achieved also in heat-affected zones caused by the welding. In this study the heat-affected zones were created using the physical simulation, so that the zones would be wide enough for reliable mechanical testing.

Continuous cast 500 MPa offshore steel was hot rolled in the laboratory hot rolling mill to find out the mechanical properties of the base metal. The physically simulated heat-affected zones were studied using Gleeble 3800. Two different cooling times from 800 °C to 500 °C ($t_{8/5}$) were used in order to simulate two different welding methods with different heat inputs. Microstructure of both base materials and simulated heat-affected zones were studied using scanning electron microscope and laser scanning confocal microscope. Charpy V-notch impact toughness and hardness profiles were determined of both base material and simulated heat-affected zones.

The base metal microstructure was ferritic with some lath-like bainitic features. Minor changes were noted in the microstructure of physically simulated inter-critical heat-affected zone (ICHAZ), while in physically simulated coarse grained heat-affected zone (CGHAZ) the prior austenite grains had coarsened and the transformation microstructure consisted of lath-like features of bainite and in case of a shorter $t_{8/5}$ of 6 s, even martensite. It was found out that the critical location regarding the impact toughness in arctic temperatures was found out to be CGHAZ, while the impact toughness of ICHAZ did not differ remarkably from that of the base material. The CGHAZ impact toughness was weaker with $t_{8/5}$ = 30 s than with $t_{8/5}$ = 6 s indicating that lower heat input welding methods are more beneficial for this material.

Keywords: Physical Simulation, CGHAZ, Impact Toughness, Welding simulation.

1 Introduction

The demand for the offshore steels with excellent properties in harsh arctic conditions is increasing steadily as the oil and gas resources of Arctic Sea are being discovered and harnessed. The well-known fact is that often the weakest location in steel structures can be traced to the welded joints and especially to different heat affected zones (HAZ) in the parent material caused by the thermal cycles of welding. Due to practical difficulties in studying the HAZ, i.e. the narrow width of each HAZ makes their testing difficult, physical simulation of HAZ provides a good tool to study their mechanical properties. By adjusting the parameters, it is also possible to simulate relatively easily different heat inputs. In recent years physical simulation of HAZ has been used successfully in various studies [1–4].

Therefore, aim of the present study is to compare the mechanical properties, especially impact toughness, of different physically simulated HAZ to each others and to the base material that was not exposed to the heat input. Further, the aim is to find out what is the critical HAZ regarding the low temperature impact toughness in the studied steel and to discuss its impact on service properties.

2 Experimental

The studied base material was an experimental continuous cast 500 MPa offshore steel designed for the arctic conditions. This type of steel is used mainly for constructing different kind of parts for the offshore oil-drilling platforms operated in extremely cold conditions. Besides that, the steel may be used in various other applications i.e. ships and other vehicles designed to operate in arctic conditions. The C-content of the steel was 0.07% and the calculated carbon equivalent value (CEV) was 0.35, and therefore means that the steel has good weldability according the Graville diagram [5]. Pieces of the cast were hot rolled to the thickness of 8 mm using a laboratory scale rolling mill. The target finishing roll temperature was 820 °C after which the steel was targeted to cool to 400 °C with the cooling rate of 30 °C/s. After that the steel was left to cool to room temperature by air.

Welding zones were simulated using Gleeble 3800. Four different thermal cycles were performed to simulate inter-critical heat-affected zone (ICHAZ) and coarse-grained heat-affected zone (CGHAZ) by flux cored arc welding (FCAW) and submerged arc welding (SAW) methods according Table 1. Rykalin 2D model [6] was used for the simulation of the heat-affected zones.

ICHAZ and CGHAZ were chosen for simulation because ICHAZ tends to be prone to softening and CGHAZ is known to has weak toughness. The softening of ICHAZ has been reported for example in the investigations of Martinez et al. [7] and Zhang et al. [8]. They investigated the welding of high strength compositions and reported that the softest zone of HAZ locates in the IC zone, where the soft tempered ferritic microstructure surrounded the martensite-retained austenite (MA) constituents.

FCAW and SAW welding methods were chosen because they are required by the standard EN10225 [9] "Weldable structural steels for fixed offshore structures - Technical delivery conditions". This European Standard specifies requirements for weldable structural steels to be used in the fabrication of fixed offshore structures.

Table 1. Gleeble-simulated welding zones and their peak temperature (T_p) and cooling time from 800 °C to 500 °C.

Heat affected zone	T_p	$t_{8/5}$	Simulated welding method
ICHAZ	750 °C	6 s	FCAW
ICHAZ	750 °C	30 s	SAW
CGHAZ	1350 °C	6 s	FCAW
CGHAZ	1350 °C	30 s	SAW

Microstructure of the base material and simulated HAZ was characterized using a Zeiss Sigma field emission scanning electron microscope (FESEM) operated at 5 kV and a Keyence VK-X200 laser scanning confocal microscope (LSCM) after Nital etching.

Hardness was measured using a Duramin-A300 (Struers) under a 100 N load (HV10) from the centreline and TD-ND surface of the base material and along HAZ simulated samples. Three flat tensile testing specimens (8x25x235 mm) according SS-standard in longitudinal direction were prepared from the base material. Impact toughness of base material and HAZ samples were tested by Charpy V-notch testing for 5x10x55 mm specimens transverse to rolling direction.

3 Results and discussion

3.1 Base material

The typical microstructure of the base material is presented in the Fig. 1. Microstructure consisted of mainly polygonal ferrite, although the minor fraction of bainitic structures are also present.

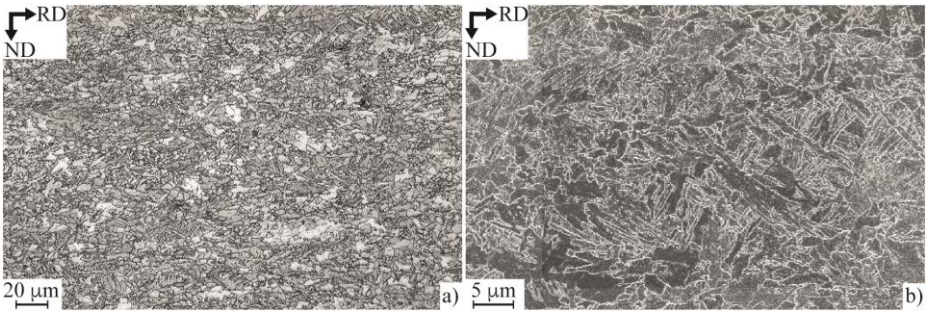

Fig. 1. LSCM (a) and SEM (b) images of the base metal microstructure in the studied steel. The images are taken from the ¼ thickness of the laboratory hot rolled plates.

The hardness and tensile testing results of the base material are presented in Table 2. Charpy V-notch impact toughness testing results of the base material are presented together with the results of physically simulated ICHAZ and CGHAZ in Figs. 4 and 7, respectively. The achieved properties were as desired and typical for the 500 MPa offshore steels.

Table 2. Mechanical properties of the base material. The deviations are defined as 95% confidence interval using student-t method.

Hardness (HV10)	Yield strength (MPa)	Ultimate tensile strength (MPa)	Elongation (%)
201±3	494±12	609±7	26.2±2.2

3.2 HAZ simulated samples

ICHAZ

Gleeble-simulated ICHAZ microstructures with $t_{8/5}$ = 6 s and $t_{8/5}$ = 30 s are presented in Figs. 2a-b and Figs. 2c-d, respectively. In ICHAZ, the material has partly austenitezed during the thermal cycle. In the other part, the phases have remained in their original form. However, due to thermal activation, partitioning of carbon to the austenite and segregation of other elements to grain boundaries is expected to take place. MA-constituents seem to be present especially in the image of ICHAZ with $t_{8/5}$ = 30 s in Figs. 2c & 2d, as they have had more time to grow during the slower cooling time.

The microstructures of ICHAZ in FESEM images in Figs. 2b and 2d look like polygonal ferrite or possibly granular bainite. MA-constituents might be seen in the grain boundaries. Clear differences with the cooling times are difficult to see. In both images nanoscale precipitates are present inside the grains. They can be either carbides or nitrides. However, they are unable to be characterized without proper transmission electron microscopy.

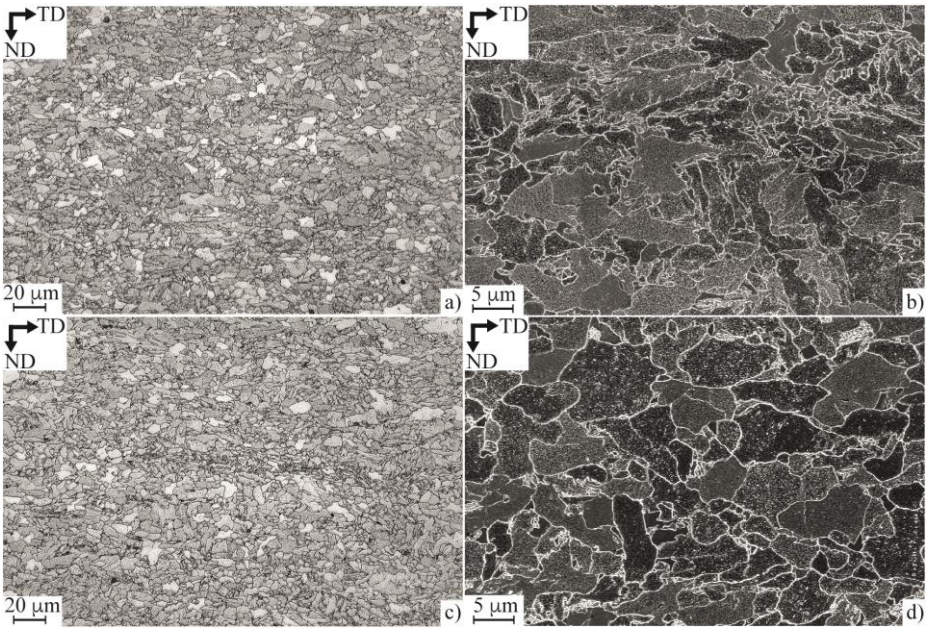

Fig. 2. LSCM images of ICHAZ with $t_{8/5}$ = 6 s (a) and $t_{8/5}$ = 30 s (c) as well as FESEM images of ICHAZ with $t_{8/5}$ = 6 s (b) and $t_{8/5}$ = 30 s (d).

Hardness measurement results over the Gleeble-simulated ICHAZ surfaces in the studied steel are presented in Fig. 3. It can be seen that hardness values in ICHAZ were approx. 190-210HV that are not notable differences comparing to the base material. Unlike in previous studies [7,8] with higher strength, the hardness of ICHAZ was not softened in the current study. That is likely due to the lower strength of the steel matrix than in the studies mentioned above.

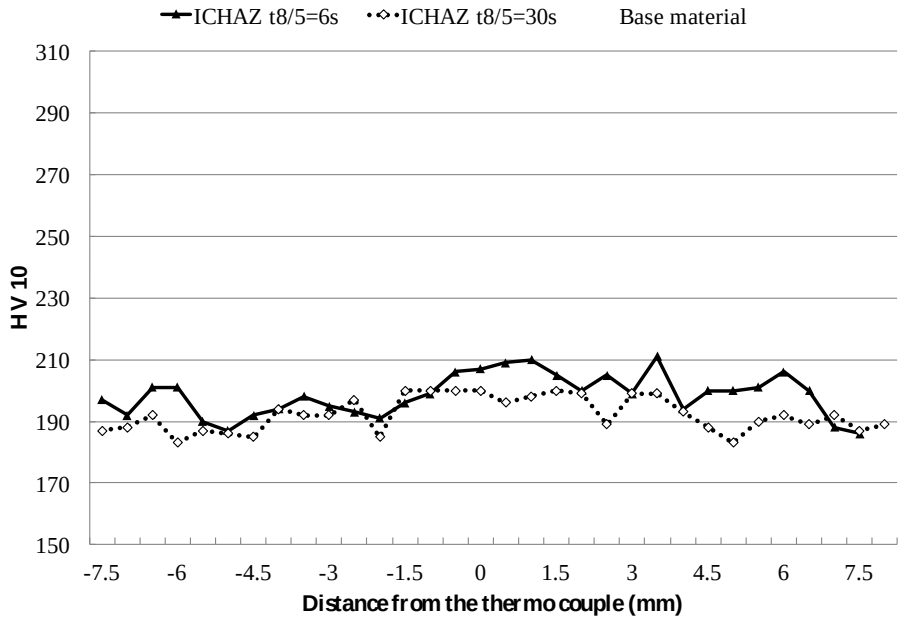

Fig. 3. Hardness over the physically simulated ICHAZ surfaces in the studied steel.

Charpy V-notch impact toughness results of physically simulated ICHAZ together with the results of the base material are presented in Fig. 4. It can be seen that the impact toughness of ICHAZ did not differ of that of the base material and remained in the upper shelf still approximately at -40 °C. The difference in $t_{8/5}$ did not show remarkable effect on the results. In higher strength steels it is expected that the brittle M/A particles would deteriorate the impact toughness of ICHAZ. However, in the current study the softer steel matrix than in high strength steels is not so greatly prone to the impact toughness problems by brittle particles.

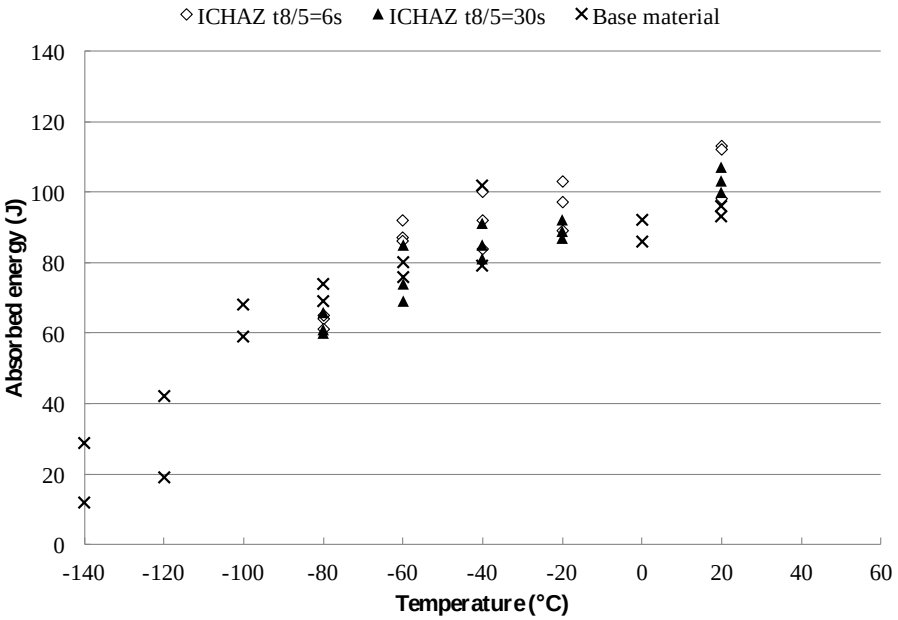

Fig. 4. Charpy V-notch impact toughness testing results of the physically simulated ICHAZ and the base material of the studied steel.

CGHAZ

The samples were fully austenitized during the CGHAZ simulation. The LSCM images of the CGHAZ in Figs. 5a and 5c shows that the prior austenite grains were coarsened and the microstructure consisted of various bainite morphologies, i.e. granular, upper and lower bainite. The FESEM images of CGHAZ microstructures, in Figs. 5b and 5d, provide more accurate observations of the microstructures. It is visible that nanoscale precipitates were still present within the grains, but less pronouncedly than in ICHAZ. This was expected due to the dissolution of precipitates at the CGHAZ simulation temperatures. That in turn increases the prior austenite grain growth during the austenitizing. With slower cooling time ($t_{8/5}$ = 30 s) microstructure consisted of granular, upper and lower bainite and, whereas simulation with the faster cooling time $t_{8/5}$ = 6 s consisted mainly of lower bainite and a small fraction of martensite. Such a hardened microstructure is the result of fast cooling rate but also the increased prior austenite grain size that enhances the hardenability, even if the carbon content of the steel is relatively low. The obtained microstructures match with the ones in a previous study [10].

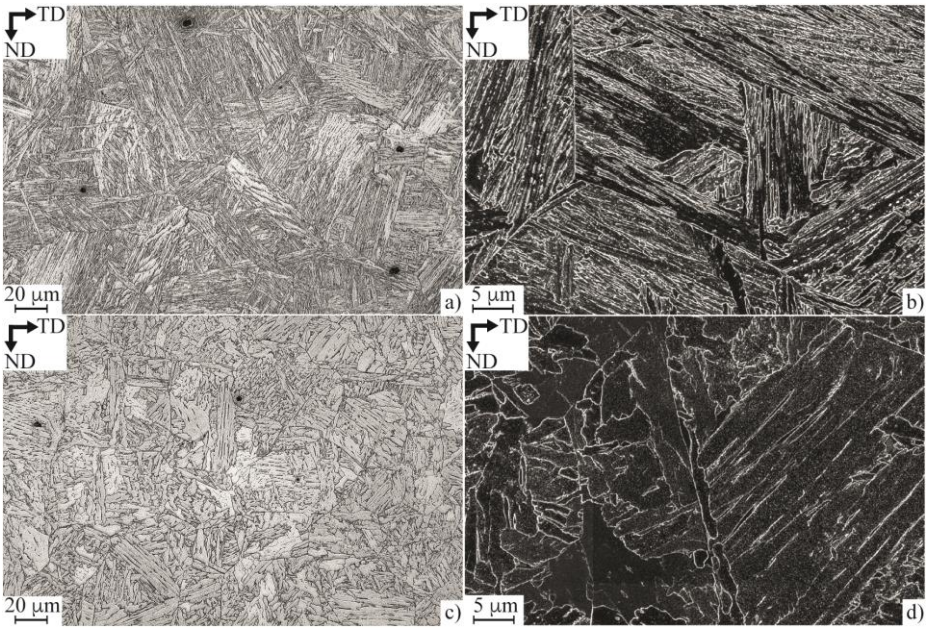

Fig. 5. LSCM images of CGHAZ with $t_{8/5}$ = 6 s (a) and $t_{8/5}$ = 30 s (c) as well as FESEM images of CGHAZ with $t_{8/5}$ = 6 s (b) and $t_{8/5}$ = 30 s (d).

Hardness measurement results over the Gleeble-simulated CGHAZ surfaces in the studied steel are presented in Fig. 6. It can be seen that the hardness increased in CGHAZ with $t_{8/5}$=6 s, whereas in CGHAZ with $t_{8/5}$=30 s there were no notable differences in hardness comparing to the base material. The increase of the hardness in CGHAZ with faster cooling rate can be explained by the lath-type microstructure, as can be seen in Fig. 5.

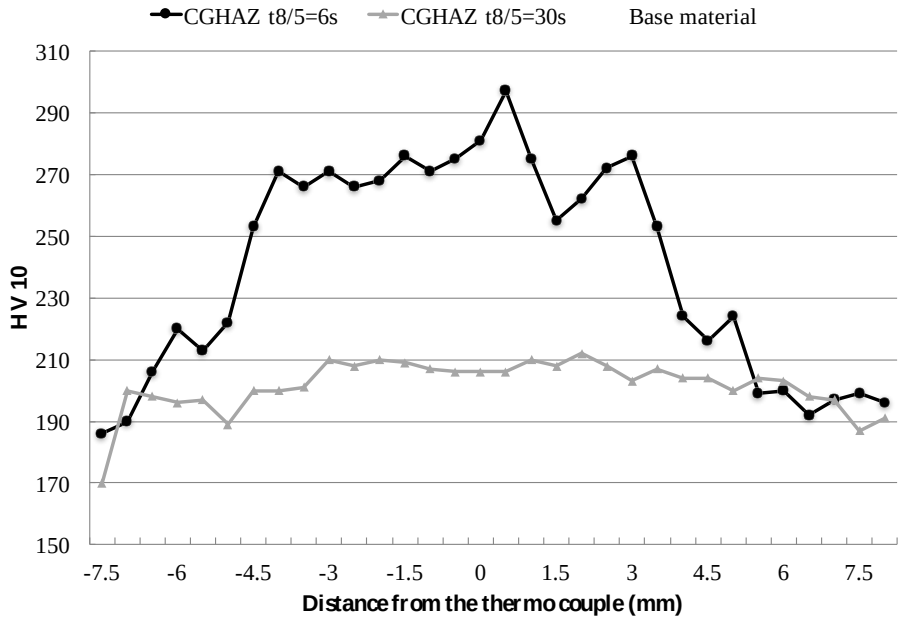

Fig. 6. Hardness over the physically simulated CGHAZ surfaces in the studied steel.

Charpy V-notch impact toughness results of physically simulated CGHAZ together with the results of the base material are presented in Fig. 7. It can be seen that the upper shelf energies were generally even a bit higher than in base material samples. On the other hand, the drop to the lower shelf was dramatic especially in samples with $t_{8/5}$ = 30 s, which behaved brittle already at -40 °C. With $t_{8/5}$ = 6 s the impact toughness was still good at -40 °C. However, at lower temperatures some of the samples fractured brittle and the absorbed energy was very low, while at the same temperature other samples fractured still ductile having high absorbed energy. This scattering could be explained by inclusions present in the steel, by single coarse grains or by the common effect of them [11]. On the other hand, the difference could be partly due to a normal scattering in ductile-brittle transition temperature (DBTT) zone. That suggests that the DBTT has increased in the CGHAZ compared to ICHAZ and base material.

Generally, it can be seen that the impact toughness of ICHAZ and CGHAZ followed the same trend with that of the base material until in lower temperatures from -40 °C the CGHAZ samples with $t_{8/5}$ = 30 s started showing reduced results. The decreased impact toughness of CGHAZ compared to HAZ further from the fusion line was also observed in a previous study by Mourujärvi et al. [12]. However, with $t_{8/5}$ = 6 s the impact toughness did not start to deteriorate until at -60 °C and even at -80 °C single samples provided good impact toughness. According to this observation, it seems that the low heat input welding with faster cooling works better with the studied steel. The reason for the better impact toughness in CGHAZ with $t_{8/5}$ = 6 s may be due to the lower bainitic microstructure that enhances both strength and toughness. Additionally, the CGHAZ with $t_{8/5}$ = 30 s is more likely to have a greater fraction of brittle M/A particles

than the CGHAZ with $t_{8/5}$ = 6 s deteriorating the impact toughness as was observed in a study with similar steel composition and cooling rates [10].

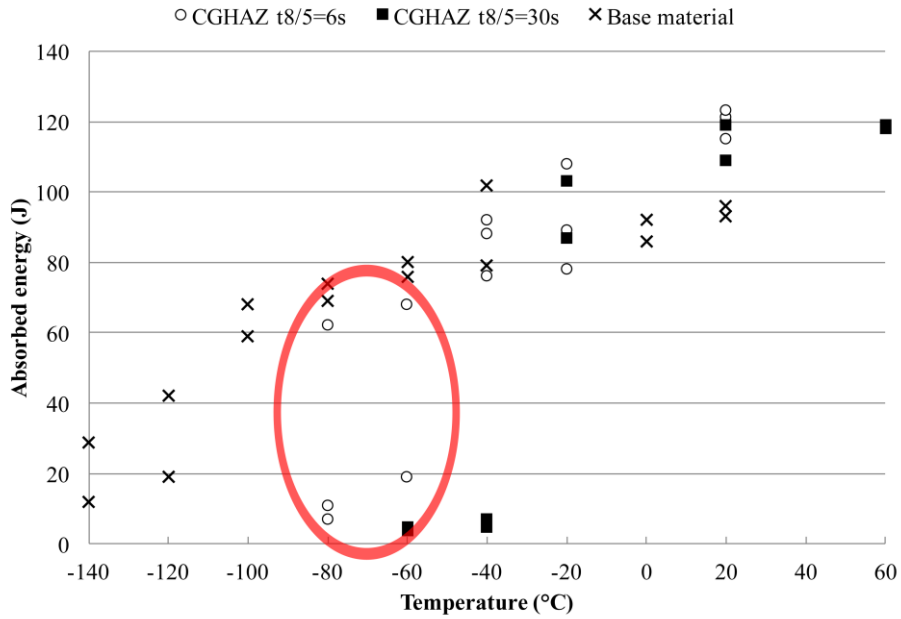

Fig. 7. Charpy V-notch impact toughness testing results of the physically simulated CGHAZ and the base material of the studied steel. Ductile-brittle transition temperature zone of the CGHAZ with $t_{8/5}$ = 6 s is marked by a red ellipse.

In this work, it was shown that especially the CGHAZ has remarkably lower impact toughness than the base material in the studied 500 MPa offshore steel. Generally, the weld joints are the weakest spots in structures and this should be considered when designing and manufacturing structures by making sure that the highest stresses are not directed to the weld joints.

4 Summary

In this study, the physically simulated ICHAZ and CGHAZ with two different cooling time $t_{8/5}$ were studied and compared. The studied steel was experimental 500 MPa offshore steel designed for arctic conditions that was hot rolled to the thickness of 8 mm by a laboratory scale hot rolling mill. The following observations and conclusions were summarized:

– The microstructure of the studied steel consisted of bainite and ferrite in the base material and ICHAZ, while even martensite in the CGHAZ with $t_{8/5}$ = 6 s.

- Impact toughness of base material and ICHAZ was relatively good, but the critical location in the studied material was found out to be in CGHAZ.
- The weakest impact toughness of CGHAZ was when $t_{8/5}$ was 30 s. However, this material showed better impact toughness of CGHAZ when $t_{8/5}$ was 6 s. This indicates that using lower heat input welding methods is beneficial with the studied steel.
- The reason for the improved impact toughness in the CGHAZ with $t_{8/5}$ = 6 s compared to that of $t_{8/5}$ = 30 s was suggested to be the lower bainitic microstructure together with the low number of brittle M/A particles.

Acknowledgement

The authors are grateful to the Finnish Funding Agency for Technology and Innovation (Tekes) for financing this work as a part of the research project FLEX – Flexible and Adaptive Operations in Metal Production. We would also like to thank the staff of the Research Center of SSAB Europe Oy Raahe for valuable cooperation.

References

[1] M. Gáspár, A. Balogh, I. Sas, Physical simulation aided process optimisation aimed sufficient HAZ toughness for quenched and tempered AHSS, in: IIW Int. Conf. High-Strength Mater. - Challenges Appl., IIW, Helsinki, Finland, 2015.

[2] S.G. Lee, D.H. Lee, S.S. Sohn, W.G. Kim, K.-K. Um, K.-S. Kim, S. Lee, Effects of Ni and Mn addition on critical crack tip opening displacement (CTOD) of weld-simulated heat-affected zones of three high-strength low-alloy (HSLA) steels, Mater. Sci. Eng. A. 697 (2017) 55–65. doi:10.1016/j.msea.2017.04.115.

[3] R. Laitinen, D.A. Porter, L.P. Karjalainen, P. Leiviskä, J. Kömi, Physical Simulation for Evaluating Heat-Affected Zone Toughness of High and Ultra-High Strength Steels, Mater. Sci. Forum. 762 (2013) 711–716. doi:10.4028/www.scientific.net/MSF.762.711.

[4] S.J. Heikkilä, D.A. Porter, L.P. Karjalainen, R.O. Laitinen, S.A. Tihinen, P.P. Suikkanen, Hardness Profiles of Quenched Steel Heat Affected Zones, Phys. Numer. Simul. Mater. Process. Vii. 762 (2013) 722–727. doi:10.4028/www.scientific.net/MSF.762.722.

[5] B.A. Graville, Cold Cracking in Welds in HSLA Steels, in: Weld. HSLA Struct. Steels, AIM/ASM, Rome, Italy, 1976.

[6] N.N. Rykalin, Calculations Concerned with Thermal Processes in Welding, Mashgiz, Moscow, 1951.

[7] E.L. Martinez, O. Vázguez-Gómez, H.J. Vergara-Hernández, S. Serna, B. Campillo, Mechanical Characterization of the Welding of Two Experimental HSLA Steels by Microhardness and Nanoindentation Tests, Met. Steels Int. 22 (2016) 987–994.

[8] L. Zhang, T. Kannengiesser, HAZ Softening in Nb-, Ti- and Ti + V -Bearing

Quenched and Tempered Steels, Weld. World. 60 (2016) 177–184.
[9] EN 10225, Weldable Structural Steels for Fixed Offshore Structures. Technical Delivery Conditions, Suomen standardoimisliitto, 2009.
[10] I.D.G. Robinson, Grain growth and austenite decomposition in two niobium containing line pipe steels, The University of British Columbia, 2016. doi:10.14288/1.0308782.
[11] A. Ghosh, A. Ray, D. Chakrabarti, C.L. Davis, Cleavage initiation in steel: Competition between large grains and large particles, Mater. Sci. Eng. A. 561 (2013) 126–135. doi:10.1016/j.msea.2012.11.019.
[12] J. Mourujärvi, S. Tihinen, S. Mehtonen, T. Lahtinen, P. Vilaca, A. Kaijalainen, D. Porter, J. Kömi, Effect of Titanium on the Weldability of Thermomechanically Rolled High-Strength Cold-Formable Steels, in: Proc. Met. 2017 - 26th Int. Conf. Metall. Mater., Brno, Czech Republic, 2017.